

University of Wollongong

## Research Online

---

Faculty of Engineering and Information  
Sciences - Papers: Part A

Faculty of Engineering and Information  
Sciences

---

1-1-2013

### **I-125 ROPES eye plaque dosimetry: Validation of a commercial 3D ophthalmic brachytherapy treatment planning system and independent dose calculation software with GafChromic EBT3 films**

Joel Poder

*Prince of Wales Hospital*, jp132@uow.edu.au

Stephanie Corde

*Prince of Wales Hospital*, scorde@uow.edu.au

Follow this and additional works at: <https://ro.uow.edu.au/eispapers>



Part of the [Engineering Commons](#), and the [Science and Technology Studies Commons](#)

---

#### **Recommended Citation**

Poder, Joel and Corde, Stephanie, "I-125 ROPES eye plaque dosimetry: Validation of a commercial 3D ophthalmic brachytherapy treatment planning system and independent dose calculation software with GafChromic EBT3 films" (2013). *Faculty of Engineering and Information Sciences - Papers: Part A*. 1919. <https://ro.uow.edu.au/eispapers/1919>

Research Online is the open access institutional repository for the University of Wollongong. For further information contact the UOW Library: [research-pubs@uow.edu.au](mailto:research-pubs@uow.edu.au)

---

# **I-125 ROPES eye plaque dosimetry: Validation of a commercial 3D ophthalmic brachytherapy treatment planning system and independent dose calculation software with GafChromic EBT3 films**

## **Abstract**

**Purpose:** The purpose of this study was to measure the dose distributions for different Radiation Oncology Physics and Engineering Services, Australia (ROPES) type eye plaques loaded with I-125 (model 6711) seeds using GafChromic R EBT3 films, in order to verify the dose distributions in the Plaque Simulator<sup>TM</sup> (PS) ophthalmic 3D treatment planning system. The brachytherapy module of RADCALC R was used to independently check the dose distributions calculated by PS. Correction factors were derived from the measured data to be used in PS to account for the effect of the stainless steel ROPES plaque backing on the 3D dose distribution. **Methods:** Using GafChromic R EBT3 films inserted in a specially designed Solid Water<sup>TM</sup> eye ball phantom, dose distributions were measured three-dimensionally both along and perpendicular to I-125 (model 6711) loaded ROPES eye plaque's central axis (CAX) with 2 mm depth increments. Each measurement was performed in full scatter conditions both with and without the stainless steel plaque backing attached to the eye plaque, to assess its effect on the dose distributions. Results were compared to the dose distributions calculated by Plaque Simulator<sup>TM</sup> and checked independently with RADCALC R. **Results:** The EBT3 film measurements without the stainless steel backing were found to agree with PS and RADCALC R to within 2% and 4%, respectively, on the plaque CAX. Also, RADCALC R was found to agree with PS to within 2%. The CAX depth doses measured using EBT3 film with the stainless steel backing were observed to result in a 4% decrease relative to when the backing was not present. Within experimental uncertainty, the 4% decrease was found to be constant with depth and independent of plaque size. Using a constant dose correction factor of  $T = 0.96$  in PS, where the calculated dose for the full water scattering medium is reduced by 4% in every voxel in the dose grid, the effect of the plaque backing was accurately modeled in the planning system. Off-axis profiles were also modeled in PS by taking into account the three-dimensional model of the plaque backing. **Conclusions:** The doses calculated by PS and RADCALC R for uniformly loaded ROPES plaques in full and uniform scattering conditions were validated by the EBT3 film measurements. The stainless steel plaque backing was observed to decrease the measured dose by 4%. Through the introduction of a scalar correction factor (0.96) in PS, the dose homogeneity effect of the stainless steel plaque backing was found to agree with the measured EBT3 film measurements.

## **Keywords**

calculation, software, gafchromic, ophthalmic, ebt3, brachytherapy, films, 3d, treatment, commercial, planning, validation, system, dosimetry, plaque, independent, eye, dose, ropes, 125, i

## **Disciplines**

Engineering | Science and Technology Studies

## **Publication Details**

Poder, J. & Corde, S. (2013). I-125 ROPES eye plaque dosimetry: Validation of a commercial 3D ophthalmic brachytherapy treatment planning system and independent dose calculation software with GafChromic EBT3 films. *Medical Physics*, 40 (12), 121709-1-121709-11.

## **I-125 ROPES eye plaque dosimetry: validation of a commercial 3-D ophthalmic brachytherapy treatment planning system and independent dose calculation software with GafChromic<sup>®</sup> EBT3 films.**

Joel Poder and Stéphanie Corde

Department of Radiation Oncology, Prince of Wales Hospital, Randwick, NSW, Australia, 2031

**Purpose:** The purpose of this study was to measure the dose distributions for different Radiation Oncology Physics and Engineering Services Australia (ROPES) type eye plaques loaded with I-125 (model 6711) seeds using GafChromic<sup>®</sup> EBT3 films, in order to verify the dose distributions in the Plaque Simulator<sup>™</sup> (PS) ophthalmic 3-D treatment planning system. The brachytherapy module of RADCALC<sup>®</sup> was used to independently check the dose distributions calculated by PS. Correction factors were derived from the measured data to be used in PS to account for the effect of the stainless steel ROPES plaque backing on the 3-D dose distribution.

**Method:** Using GafChromic<sup>®</sup> EBT3 films inserted in a specially designed Solid Water<sup>™</sup> eye ball phantom, dose distributions were measured three-dimensionally both along and perpendicular to I-125 (model 6711) loaded ROPES eye plaque's central axis (CAX) with 2 mm depth increments. Each measurement was performed in full scatter conditions both with and without the stainless steel plaque backing attached to the eye plaque, to assess its effect on the dose distributions. Results were compared to the dose distributions calculated by Plaque Simulator<sup>™</sup> and checked independently with RADCALC<sup>®</sup>.

**Results:** The EBT3 film measurements without the stainless steel backing were found to agree with PS and RADCALC<sup>®</sup> to within 2% and 4% respectively, on the plaque CAX. Also, RADCALC<sup>®</sup> was found to agree with PS to within 2%. The CAX depth doses measured using EBT3 film with the stainless steel backing were observed to result in a 4% decrease relative to when the backing was not present. Within experimental uncertainty, the 4% decrease was found to be constant with depth and independent of plaque size. Using a constant dose correction factor of  $T=0.96$  in PS, where the calculated dose for the full water scattering medium is reduced by 4% in every voxel in the dose grid, the effect of the plaque backing was accurately modelled in the planning system. Off-axis profiles were also modelled in PS by taking into account the three-dimensional model of the plaque backing.

**Conclusion:** The dose calculated by PS and RADCALC for uniformly loaded ROPES plaques in full and uniform scattering conditions were validated by the EBT3 film measurements. The stainless steel plaque backing was observed to decrease the measured dose by 4%. Through the introduction of a scalar correction factor (0.96) in PS, the dose homogeneity effect of the stainless steel plaque backing was found to agree with the measured EBT3 film measurements.

## I. INTRODUCTION

Choroidal melanoma is the most common primary intraocular malignancy<sup>1</sup> and is commonly treated using external beam charged particle therapy or eye plaque brachytherapy. In 1985 the Collaborative Ocular Melanoma Study (COMS) trial<sup>2, 3</sup> compared enucleation against a minimum of 100 Gy I-125 plaque radiation therapy for medium sized choroidal melanomas (2.5 – 10 mm in height and a maximum basal dimension of 16 mm), showing no significant difference in survival<sup>4</sup>. The COMS trial's protocol calculated doses using a point source approximation and no heterogeneity correction.

Following the publication of AAPM TG-43 report in 1995 providing a dose calculation formalism for Ir-192, I-125 and Pd-103 sources<sup>5</sup> and the changes to a new primary air kerma strength calibration standard<sup>6</sup>, the recommended dose prescription of 100 Gy was lowered to 85 Gy. This new dose calculation formalism allowed for a line source approximation of the source; however the effects of the plaque backing and seed carrier were still ignored. A TG-43 report update was released in 2004 (TG-43U1)<sup>7</sup> to include new brachytherapy sources and critically reassess some published brachytherapy dosimetry data including the I-125 source (Amersham Health (Princeton, NJ) model 6711). Recommendations were also provided for dose calculation methods for episcleral plaque therapy following the COMS protocol.

It is now well recognized that incorporating the effects of heterogeneities into the dose calculation is essential and can result in a significant change in the dose to the tumour and sensitive structures in episcleral plaque therapy. This has been an area of extensive research in recent years, using both experimental<sup>8-11</sup> and Monte Carlo methods<sup>1, 12-14</sup>. This is reflected in the recent release of the AAPM TG-129 report<sup>15</sup>, which gives recommendations for treatment planning and examines the effect of plaque heterogeneities on the dose distribution.

The TG-129 report focuses on the standard COMS design eye plaques, examining heterogeneity effects specific to this plaque design. The standard COMS plaque design consists of a gold-alloy backing (density = 15.8 g/cm<sup>3</sup>) and a Silastic seed carrier insert (density 1.12 g/cm<sup>3</sup>,  $Z_{\text{eff}} = 11$ ). ROPES type eye plaques however, consist of a stainless steel backing (density = 7.912 g/cm<sup>3</sup>) and an acrylic seed carrier insert (density 1.069 g/cm<sup>3</sup>,  $Z_{\text{eff}} = 6.5$ )<sup>16</sup>. For both the COMS and ROPES plaques the seed insert has a radius of curvature of ~12 mm in order to conform to the external sclera and offset the seeds by 1 mm from the sclera. Due to differences in atomic number and density of materials used in the construction of the ROPES and COMS type eye plaques, the effect of these materials on the dose distributions produced by the plaques is expected to be dissimilar. For example, the effective atomic number of the acrylic insert in the ROPES type eye plaques is much closer to the atomic number of water ( $Z_{\text{eff}} \sim 7.4$ )<sup>13</sup>, than that of the Silastic insert in the COMS type plaques.

Thomson and Rogers reported in 2010, that the dose calculations are specific to not only the seed model, but also the type of eye plaque<sup>1</sup>. Using the BrachyDose Monte Carlo code, they calculated dose distributions for six Pd-103 and I-125 seed models. Differences in dose reduction relative to homogeneous water assumption varied between seed models and plaque types of order 2%. Whilst the dosimetric studies of model 6711 I-125 seeds are extensive, many of these are limited to the study of the seeds in conjunction with COMS plaques<sup>1, 8, 13, 14</sup>. To date, one group has published a Monte Carlo study of the dose distributions produced by ROPES type eye plaques with model 6711 I-125 seeds<sup>17</sup>, and another using two models of Pd-103 seeds<sup>16</sup>.

Granero *et al.*<sup>17</sup> performed Monte Carlo simulations both with and without the acrylic seed carrier to assess its effect on the dose distribution for the 15 mm diameter ROPES plaque. Saidi *et al.*<sup>16</sup> also performed Monte Carlo simulations of the 15 mm diameter ROPES plaque. Using version 5 of MCNP, the effect of the stainless steel backing and acrylic carrier on the dose distributions produced by plaques loaded with Theragenics200 and IR06 Pd-103 seeds was assessed.

Whilst Monte Carlo methods are increasingly being used in the study of low energy photon emitting brachytherapy sources, experimental studies are still of value in order to address the variability that represents the clinical environment<sup>7</sup>. The low energy of the photons emitted by the I-125 seed makes experimental measurements of the dose distributions emitted by the seed particularly difficult. The steep dose gradients result in the need for the detector being used to have a relatively small active volume. The

detector also needs to be water-equivalent in the energy range of interest, or have a well-characterized energy response function.

Previous attempts to measure dose distributions produced by 10 mm and 15 mm diameter ROPES plaques using customized PRESAGE<sup>™</sup> 3-D type dosimeters<sup>18</sup> lacked accurate calibration of the fluorescence intensity measurements to dose. The small size of the customized gels prevented high resolution 3-D measurements but still demonstrated an effect of the stainless steel backing on the ROPES plaque CAX dose.

Radiochromic film dosimetry has recently been established as a reliable method in measuring dose distributions produced by COMS type eye plaques loaded with various I-125 seed models<sup>10, 19-22</sup>. Acar<sup>22</sup> and Acar *et al.*<sup>19</sup> have used GafChromic<sup>®</sup> EBT film in a polystyrene eye phantom to measure absolute doses along the plaque CAX and in off-axis directions at depths of 5 and 12 mm for four types of COMS plaques loaded with model I25.S16 I-125 seeds. Krintz *et al.*<sup>10</sup> measured relative dose distributions from COMS eye plaques uniformly loaded with model 6711 I-125 seeds in a Solid Water<sup>™</sup> phantom using GafChromic model MD55-2 films. They found a 15% average decrease of the relative off-axis doses as measured by the films compared to doses calculated by PS.

The Plaque Simulator<sup>™</sup> program is a dedicated eye plaque treatment planning system. The software supports dose calculations for a variety of radioactive nuclides and seed models. The dose calculations are performed in 3-D and are visualized on retinal diagrams and sagittal cross-sections<sup>23</sup>. The algorithm is based on the AAPM TG-43 dose calculation formalism, using the superposition of contributions to the total dose from individual seeds<sup>24</sup>. The software also incorporates additional features that could model three-dimensionally the effect of the plaque backing material and ray-trace the path of primary radiation between the calculation point and a linear radiation source. The three-dimensional model of the plaque backing material uses an algorithm that attenuates primary radiation which passes through the shape of the plaque backing, whilst ignoring all secondary scatter effects. The software accounts for collimation and scatter effects of the primary radiation emitted from the radioactive seeds by the metal plaque backing and transmission by the seed carrier through the carrier (or dose correction) factor<sup>24</sup>. These effects are well defined in COMS plaques<sup>25</sup>, however corrections for ROPES type eye plaques are yet to be adequately defined, and there are no corrections available for ROPES eye plaques in PS.

RADCALC<sup>®</sup> v6.1.3.2 (Lifeline Software, Inc. USA) is a versatile program designed to independently check radiotherapy dose calculations. The brachytherapy module calculates doses to points of interest for

various brachytherapy sources whose data and model/approximation are user defined. The brachytherapy module of the RADCALC<sup>®</sup> program has previously been shown by Dempsey<sup>26</sup> as being a useful tool for independent checking of dwell times in high dose rate brachytherapy applications. The current study aims to extend this application and use RADCALC<sup>®</sup> as an independent checking program for eye plaque brachytherapy implant times as calculated by PS.

In this work, the absolute doses for a number of ROPES type eye plaques loaded with uniform activity model 6711 I-125 seeds were calculated by both PS and RADCALC<sup>®</sup>. These calculations were experimentally verified by performing absolute dose measurements with GafChromic<sup>®</sup> EBT3 film in a specially designed Solid Water<sup>™</sup> eye phantom. These measurements were performed both with and without the stainless steel plaque backing in order to quantify the effect of the plaque backing in three-dimensions. Using the results of the film measurements, correction factors were used to model the effect of the ROPES plaque backing proposed in the PS software.

## **II. MATERIALS AND METHODS**

### **II.A. I-125 seed and ROPES eye plaques**

The ROPES eye plaques (Figure 1) consist of an acrylic carrier with slots for the I-125 seeds combined with a stainless steel backing shield to place the acrylic insert in. Available nominal diameters are 10, 15 and 18 mm with 4, 9 or 10, and 14 seeds, respectively. The 15 mm diameter plaque with the 9 seed insert is used for tumours close to the optic nerve. The stainless steel backing and the acrylic insert are portion of a semi-spherical shell and offset the radioactive seeds by approximately 1 mm from the outer sclera<sup>17</sup>.

Figure 1 shows the configuration of the seeds within each of the four different ROPES eye plaques used in this study. The angle  $\phi$  defines the angle between the positive x axis and the projection on the x-y plane of the line passing through the seed centre (as shown in Figure 1b). The seed coordinates for each eye plaque are listed in Table I. Like the TG-129 report and COMS, the coordinate system origin is defined as 1 mm away from the inner concave surface at the rotational centre of the acrylic insert, with the positive z axis pointing into the eye. The x and y axes are defined as shown in Figure 1. The seed coordinates are based on those defined in Plaque Simulator<sup>™</sup> (v 5.5.0) that were found to agree with engineering drawings

provided by the manufacturer to within 0.04 mm, with the exception of the 10 mm plaque which is a non-standard prototype ROPES eye plaque<sup>27</sup>.

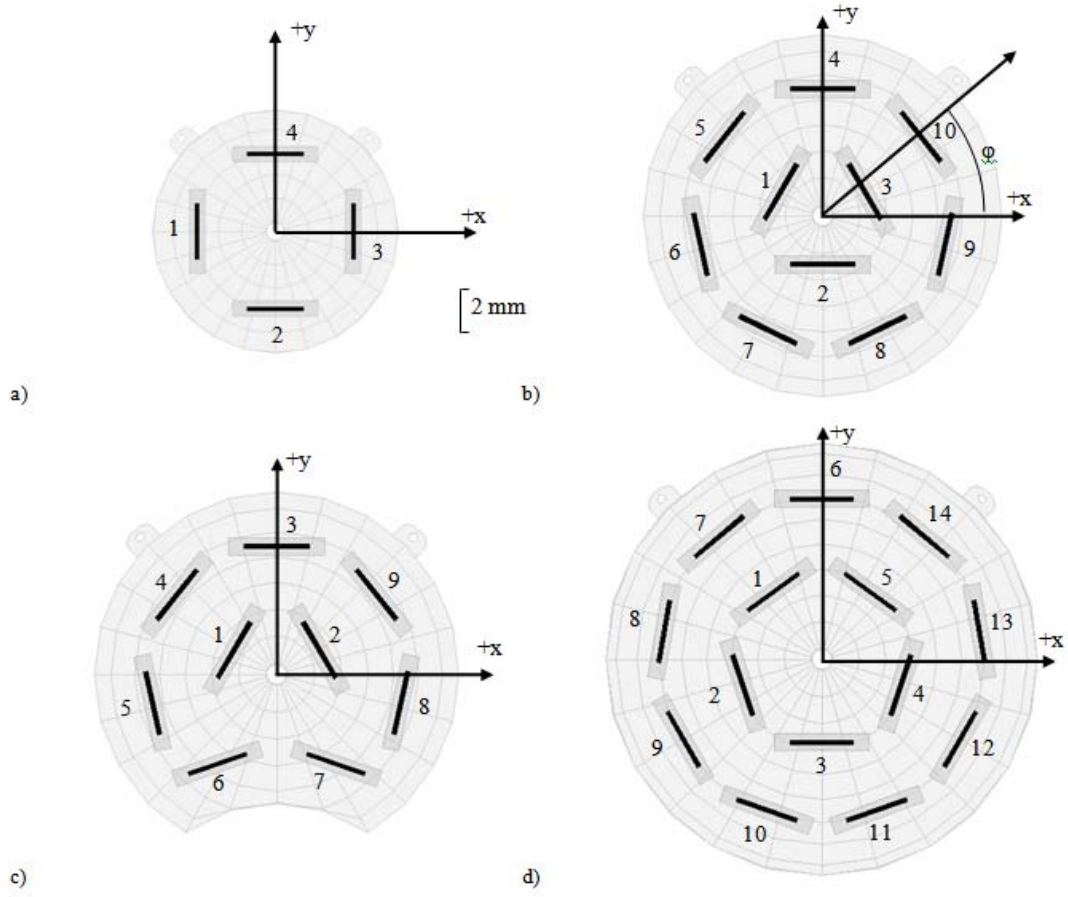


FIG. 1. Seed diagram for a) the 10 mm ROPES plaque, b) the 15 mm ROPES plaque, c) the 15 mm notched ROPES plaque, d) the 18 mm ROPES plaque. The views are from the concave aspect of the acrylic seed carrier as shown in PS, the  $+z$  axis is defined as pointing out of the page towards the centre of the eye.

TABLE I. Seed coordinates (mm) for the 10 mm, 15 mm, 15 mm notched, and 18 mm diameter ROPES eye plaques. Position of the seed numbers are shown in Figure 1. The coordinate system origin is defined as 1 mm away from the inner concave surface at the rotational centre of the acrylic insert. The angle  $\phi$  is the



angle between the positive x axis and the projection on the x-y plane from the origin to the seed centre is indicated in Figure 1. The seed physical length is taken as 4.5 mm.

	Seed #	Seed centre coordinates			Seed end coordinates						Angle
		x <sub>c</sub>	y <sub>c</sub>	z <sub>c</sub>	x <sub>1</sub>	y <sub>1</sub>	z <sub>1</sub>	x <sub>2</sub>	y <sub>2</sub>	z <sub>2</sub>	φ (°)
10*	1	-3.69	0.00	-1.99	-3.69	2.25	-1.99	-3.69	-2.25	-1.99	90.00
mm	2	0.00	-3.69	-1.99	-2.25	-3.69	-1.99	2.25	-3.69	-1.99	180.00
plaque	3	3.69	0.00	-1.99	3.69	-2.25	-1.99	3.69	2.25	-1.99	270.00
	4	0.00	3.69	-1.99	2.25	3.69	-1.99	-2.25	3.69	-1.99	0.00
15	1	-1.97	1.14	-1.9	-0.85	3.09	-1.9	-3.10	-0.81	-1.9	60.00
mm	2	0.00	-2.27	-1.9	-2.25	-2.27	-1.9	2.25	-2.27	-1.9	180.00
plaque	3	1.97	1.14	-1.9	3.10	-0.81	-1.9	0.85	3.09	-1.9	300.00
	4	0.00	5.95	-0.67	2.25	5.95	-0.67	-2.25	5.95	-0.67	0.00
	5	-4.65	3.71	-0.67	-3.25	5.47	-0.67	-6.05	1.95	-0.67	51.43
	6	-5.80	-1.32	-0.67	-6.30	0.87	-0.67	-5.30	-3.52	-0.67	102.86
	7	-2.58	-5.36	-0.67	-4.61	-4.38	-0.67	-0.55	-6.33	-0.67	154.29
	8	2.58	-5.36	-0.67	0.55	-6.33	-0.67	4.61	-4.38	-0.67	205.71
	9	5.80	-1.32	-0.67	5.30	-3.52	-0.67	6.30	0.87	-0.67	257.14
	10	4.65	3.71	-0.67	6.05	1.95	-0.67	3.25	5.47	-0.67	308.57
15	1	-1.97	1.14	-1.9	-0.85	3.09	-1.9	-3.10	-0.81	-1.9	60.00
mmN	2	1.97	1.14	-1.9	3.10	-0.81	-1.9	0.85	3.09	-1.9	300.00
plaque	3	0.00	5.95	-0.67	2.25	5.95	-0.67	-2.25	5.95	-0.67	0.00
	4	-4.65	3.71	-0.67	-3.25	5.47	-0.67	-6.05	1.95	-0.67	51.43
	5	-5.80	-1.32	-0.67	-6.30	0.87	-0.67	-5.30	-3.52	-0.67	102.86
	6	-2.77	-4.18	-1.10	-0.75	-3.47	-1.81	-4.78	-4.89	-0.40	146.50
	7	2.77	-4.18	-1.10	0.75	-3.47	-1.81	4.78	-4.89	-0.40	213.50
	8	5.80	-1.32	-0.67	5.30	-3.52	-0.67	6.30	0.87	-0.67	257.14
	9	4.65	3.71	-0.67	6.05	1.95	-0.67	3.25	5.47	-0.67	308.57

18	1	-2.32	3.19	-1.49	-0.50	4.51	-1.49	-4.14	1.86	-1.49	36.00
mm	2	-3.75	-1.22	-1.49	-4.44	0.92	-1.49	-3.05	-3.36	-1.49	108.00
plaque	3	0.00	-3.94	-1.49	-2.25	-3.94	-1.49	2.25	-3.94	-1.49	180.00
	4	3.75	-1.22	-1.49	3.05	-3.36	-1.49	4.44	0.92	-1.49	252.00
	5	2.32	3.19	-1.49	4.14	1.86	-1.49	0.50	4.51	-1.49	324.00
	6	0.00	7.61	0.34	2.25	7.61	0.34	-2.25	7.61	0.34	0.00
	7	-4.89	5.83	0.34	-3.17	7.27	0.34	-6.61	4.38	0.34	40.00
	8	-7.49	1.32	0.34	-7.10	3.54	0.34	-7.88	-0.89	0.34	80.00
	9	-6.59	-3.80	0.34	-7.71	-1.86	0.34	-5.46	-5.75	0.34	120.00
	10	-2.60	-7.15	0.34	-4.72	-6.38	0.34	-0.49	-7.92	0.34	160.00
	11	2.60	-7.15	0.34	0.49	-7.92	0.34	4.72	-6.38	0.34	200.00
	12	6.59	-3.80	0.34	5.46	-5.75	0.34	7.71	-1.86	0.34	240.00
	13	7.49	1.32	0.34	7.88	-0.89	0.34	7.10	3.54	0.34	280.00
	14	4.89	5.83	0.34	6.61	4.38	0.34	3.17	7.27	0.34	320.00

---

\* The 10 mm plaque is a non-standard prototype ROPES plaque<sup>27</sup>.

The Amersham Health (Princeton, NJ) model 6711 I-125 seed contains a cylindrically shaped silver rod on which I-125 has been coated onto the surface encased in a cylindrically symmetric titanium shell. It emits photons with a weighted mean energy of 28.37 keV, and has a physical length of 4.5 mm<sup>28</sup>.

## **II.B. GafChromic® EBT3 film**

The radiochromic films used in this study were GafChromic® EBT3 films with lot numbers A09231103 and A02061301 (Ashland Inc., Wayne, NJ, USA). The EBT3 film is comprised of an active layer containing the active component, marker dye, stabilizers and other additives that give the film a uniform response to high-energy and low-energy photons<sup>29, 30</sup>. The active layer is nominally 27 µm thick and is sandwiched between two 120 µm transparent polyester substrates. The yellow marker dye in the active layer reduces UV/light sensitivity and the polyester substrate has a special surface coating that maintains a

gap between the film surface and the glass window of a flatbed scanner in order to reduce the formation of Newton's Rings<sup>29</sup>. The films were handled according to the recommendations given in the AAPM TG 55 Report<sup>31</sup>.

### **II.B.1 Film calibration**

Calibration films were cut into 5x5 cm<sup>2</sup> square pieces and placed at the surface of a 30x30x5 cm<sup>3</sup> slab of Gammex RMI 457 Solid Water<sup>TM</sup> (Gammex Inc. Wisconsin, USA) in an orientation perpendicular to the beam CAX of a Pantak Therapax DXT 300 orthovoltage machine. Multiple sets of film were exposed to a 75 kVp, 30 mA beam (with inherent filtration of 2.0 mm Be, added filtration of 2.40 mm Al and HVL of 2.63 mm Al) to dose levels ranging from 0 to 2 Gy in 0.2 Gy increments at 50 cm focus to source distance. Each film was irradiated, one at a time, centred in 10x10 cm<sup>2</sup> field with the applicator abutting the film and phantom surface. The energy of the beam was chosen because the effective energy of the beam was evaluated using the SpekCalc simulation software<sup>32</sup> to be 30.0 keV, which is comparable to the 28.37 keV weighted mean energy of the model 6711 I-125 seed. Brown *et al.*<sup>30</sup> measured the relative sensitivity of EBT3 film in the energy range of 25 to 35 keV using synchrotron-produced monochromatic x-ray beams. The study showed that the sensitivity (net optical density (NOD) per unit dose) varied by less than 2% within the x-rays energy range of 25 – 35 keV. The output of the orthovoltage machine was calibrated using the IPEMB code of practice<sup>33</sup>.

### **II.B.2. Single seed measurements**

To confirm the correct calibration of the films, multiple pieces of film were irradiated in a Solid Water<sup>TM</sup> phantom at two distances away from the centre of a single model 6711 I-125 seed along its transverse axis (Figure 2). A groove was machined into a slab of Solid Water<sup>TM</sup> in the shape of the model 6711 I-125 seed and pieces of EBT3 film placed horizontally between slabs of Solid Water<sup>TM</sup>, one at a time. Additional pieces of Solid Water<sup>TM</sup> were placed below the seed and above the film in order to maintain full scatter conditions.

Measured doses were corrected using a Solid Water<sup>TM</sup> correction factor of 1.038 to account for the non perfect water equivalence of the Solid Water<sup>TM</sup> at these photon energies. This value is an average of the values published by Williamson<sup>34</sup>, Meigooni *et al.*<sup>35</sup> and Tailor *et al.*<sup>36</sup> who found Solid Water<sup>TM</sup> correction factors of 1.043, 1.032 and 1.040 respectively. As such, an uncertainty of 0.6% in the Solid Water<sup>TM</sup> correction factor has been used in this study.

The air-kerma strength<sup>7</sup> of the seed used was 8.11 U (cGy.cm<sup>2</sup>.h<sup>-1</sup>), and the EBT3 films were irradiated for a period of 1 hour. Measured doses were then compared against the TG-43U1 calculated doses from PS and RADCALC<sup>®</sup> for the given exposure time at depths of 2.51 and 4.51 mm (centre of seed to centre of film distance). All depths were measured using calibrated vernier scale callipers with a measurement precision of 0.01 mm. Also, as shown by Dolan *et al.*<sup>28</sup> the cylindrically shaped silver rod is free to move around within the titanium capsule of the 6711 seed by up to 0.08 mm in the seed transverse direction. The sum of these uncertainties gives the total combined uncertainty in depth approximation of 0.09 mm. Variation in EBT3 film thickness was found to be less than the measurement uncertainty of the callipers.

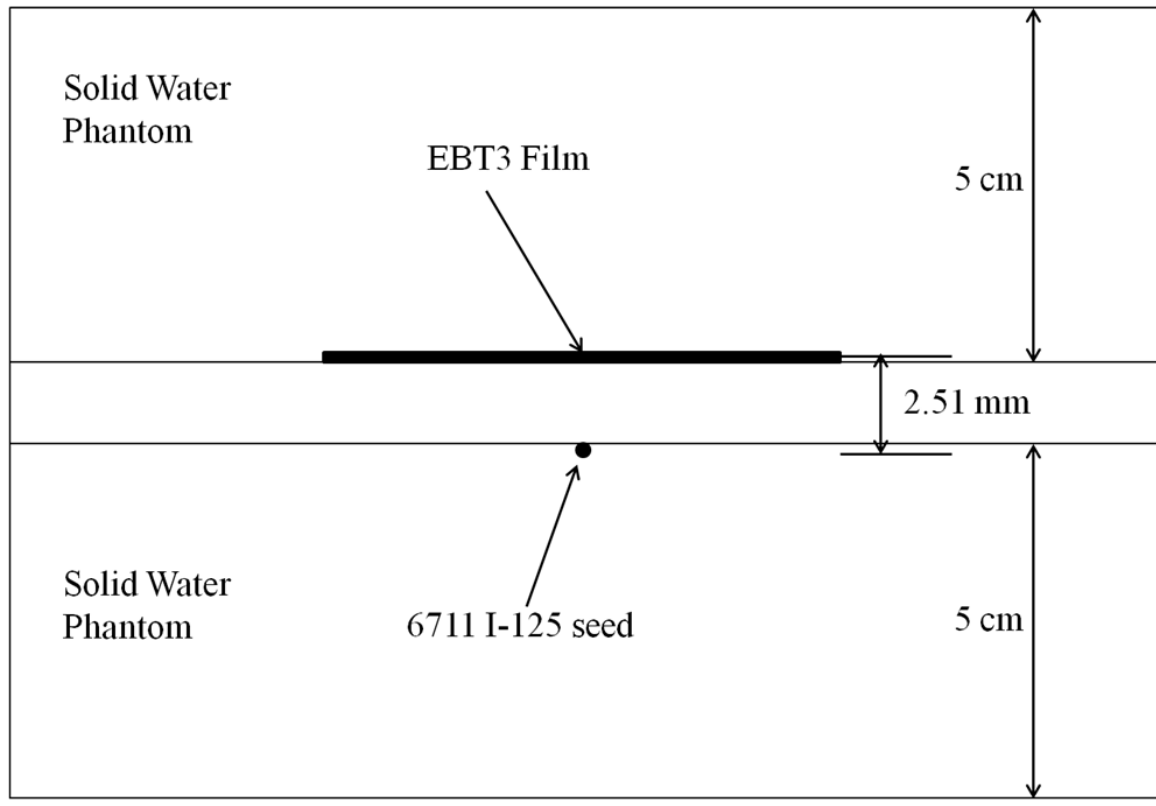


FIG. 2. Schematic diagram (not to scale) showing the configuration of the EBT3 film and I-125 seed in a Solid Water<sup>TM</sup> phantom for the single seed measurements. The reported distance is from the centre of the seed to the centre of the EBT3 film.

### **II.B.3. Eye phantom irradiations**

Experimental films were cut into 5x5 cm<sup>2</sup> square pieces and placed in a specially designed Solid Water<sup>TM</sup> eye phantom (Figure 3). The eye phantom was shaped into a sphere of 24 mm diameter and dissected into pieces of 2.00 mm thickness. The sphere could then be arranged to allow measurements with EBT3 film in increments of 2.00 mm depth with the film positioned orthogonal to the plaque CAX. A 30x30x5 cm<sup>3</sup> slab of Solid Water<sup>TM</sup> was placed beyond the EBT3 film to maintain full scatter conditions. Pieces of Solid Water<sup>TM</sup> were machined in order to fit over individual plaques, and provide full backscatter during the measurements.

ROPES eye plaques were loaded with uniform activity model 6711 I-125 seeds. EBT3 films were placed sequentially at depths of 1, 3, 5, 7 and 9 mm orthogonal to the plaque's CAX for each type of ROPES plaque. Three separate EBT3 films were used for each plaque at each measurement depth (60 in total). The exposure times were calculated in PS to deliver a total dose of 2 Gy to 2 mm depth on the plaque CAX. Seed activities used ranged from 4.6 – 9.3 U, resulting in exposure times from 0.5 – 2.5 hours.

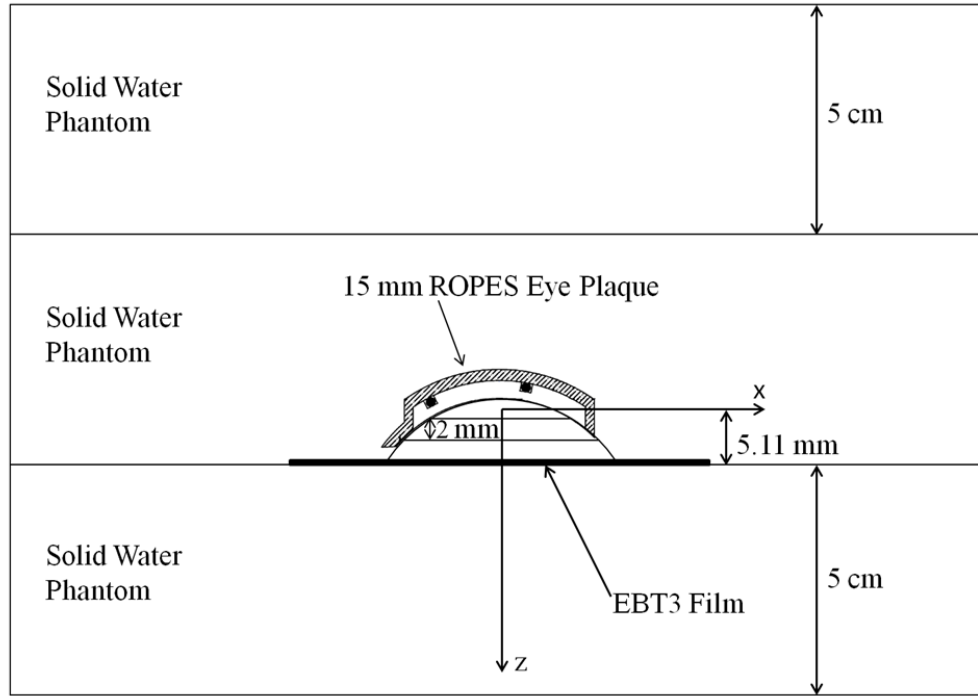


FIG. 3. Schematic diagram (not to scale) showing the experimental arrangement of the uniformly loaded ROPES eye plaque measurements. The reported distance of 5.11 mm is from the plaque origin (as described in Table I) to the centre of the EBT3 film. The 15 mm diameter ROPES plaque is shown, including the collimating lip of the plaque backing.

#### II.B.4. Film analysis & scanning

EBT3 films were scanned both prior to and 24 hours after exposure in an Epson 10000XL flatbed scanner (SEIKO Epson Co, Japan), in a jig to ensure sub-pixel reproducible positioning of the film within the scanning area. Film scans prior to exposure were obtained to measure the optical density of the background image. The post-exposure scans allowed the calculation of the net optical density (NOD) after which the latent image had stabilized<sup>37</sup> by subtracting the background value from the optical density (OD) on a per-pixel basis.

Each film was scanned in transmission mode using 48 bit RGB with a scanner resolution of 75 dpi (0.34 mm pixel size). All film pieces were marked in order to maintain the same orientation throughout scanning and measurement thereby eliminating polarisation effects<sup>38</sup>. The films were positioned at the centre

of the flatbed scanner to avoid off-axis scanner non-uniformity<sup>39</sup>. ImageJ software v1.42q (National Institutes of Health, Maryland, USA) was used to analyse films and measure pixel values for the pre-irradiation and post-irradiation scans. For calibration films, a 5x5 mm<sup>2</sup> region of interest (ROI) was used to measure the pre-irradiation and post-irradiation pixel values. Films used to measure the ROPES plaque dose distributions were analysed on a pixel by pixel basis. The pixel values measured from the red channel of the scanner were used to calculate the NOD for each film piece and these were converted to absorbed dose to water in water for I-125 ( $D_w^{I-125,w}$  in Gy) using the following formula:

$$D_w^{I-125,w} = NOD_{SW}^{I-125,films} k_{films}^{I-125,75kVp} \epsilon^{75kVp,w} F_{SW,w}$$

where

$NOD_{SW}^{I-125,films}$  is the NOD measurement of the films irradiated with I-125 in Solid Water<sup>TM</sup>;

$k_{films}^{I-125,75kVp}$  is the energy dependence of the films between I-125 and 75kVp (value taken to be 1);

$\epsilon^{75kVp,w}$  is the films NOD-to-dose to water calibration curve at 75kVp (Gy);

$F_{SW,w}$  is the solid water to water correction factor, taken as 1.038 in this study.

### II.C. Dose calculations in Plaque Simulator<sup>TM</sup> and RADCALC<sup>®</sup>

The line-source approximation for the geometry function and 2-D anisotropy corrections were used for the I-125 (model 6711) sources in both Plaque Simulator<sup>TM</sup> (v5.5.0) and RADCALC<sup>®</sup> (v6.1.3.2) and lead to single seed dose comparison of difference less than 1% at distances up to 1cm from the seed centre<sup>18</sup>.

The plaques were loaded with model 6711 I-125 seeds and treatment times calculated in PS to deliver 2 Gy to a depth of 2 mm without accounting for any plaque heterogeneity effects. In RADCALC<sup>®</sup>, the 3-D I-125 seeds geometries were defined for every ROPES eye plaque type available, as per the coordinates in Table I. The corresponding PS treatment times were corrected to take into account that RADCALC<sup>®</sup> (v6.1.3.2) does not account for the decay of the sources during treatment. CAX depth dose and off-axis dose distributions were then compared for each of the ROPES eye plaques under full homogeneous conditions, as well as to measurements made with the EBT3 film at depths of 1, 3, 5, 7 and 9 mm without the stainless steel plaque backing. A repeat of these measurements with the stainless steel backing allowed the calculation of the dose correction factor to be implemented in PS to account for the collimation and scatter

effects caused by the stainless steel backing. The three-dimensional shape of the plaque backing was modeled independently in PS according to the manufacturer's engineering drawings and depth doses and off axis profiles were recalculated with PS.

## **II.D. Uncertainty Analysis**

The calculation of the total uncertainty in the film measurements follows recommendations given in the joint AAPM/ESTRO TG 138 Report<sup>40</sup>. Components of measurement uncertainty may be classified into random uncertainties evaluated by statistical methods (type A) and those evaluated by other means, which are systematic (type B). The contributions to the total uncertainty in the calibration film measurements include a 0.8% type A uncertainty from the standard deviation of OD value within the ROI for one calibration film, a 3.5% type A uncertainty from the standard deviation of OD in repeated scanning of the same calibration film, 0.74% type B uncertainty from the fit of the curve used to convert NOD to dose and a 2.5% type B uncertainty in the calibration of the x-ray beam used to calibrate the films. The total uncertainty in conversion from NOD to dose is stated as 4.4% ( $k = 1$ ). This uncertainty in conversion from NOD to dose becomes a Type B uncertainty for eye phantom measurements.

The total uncertainty of the single seed verification measurements with three repeated measurements at each depth was estimated as 6.1%. The single type A contribution to the total uncertainty is the standard deviation of the average value of NOD from repetitive measurements. Type B contributions to the total uncertainty of the single seed measurements include, conversion of NOD to dose, uncertainty in the seed's air-kerma strength, uncertainty in the Solid Water<sup>TM</sup> correction factor used<sup>34</sup>, and seed-film positioning uncertainty.

Table II shows the estimation of the total uncertainty in the eye phantom measurements. The dosimetric effect of the positional uncertainty has been averaged over all central axis depths and plaque types. The eye phantom measurements total uncertainties are an average of 5.4% for CAX measurements and 6.7% for off-axis values.

TABLE II. Uncertainty in eye phantom measurements.



	Type A	Type B
Uncertainty in NOD from 3 data points (3 repetitive measurements).	2.5% (CAX)	
Uncertainty in NOD from 3 data points (3 repetitive measurements).	4.7% (off-axis)	
Uncertainty in conversion from NOD to dose		4.4%
Uncertainty in seed's air-kerma strength, $S_K$ , (incorporating uncertainty in half-life)		1.6%
Uncertainty in Solid Water <sup>TM</sup> correction factor		0.6%
Average positioning uncertainty, $u_d = 0.09$ mm (dose change between $d$ and $d \pm u_d$ )		0.6%
Total plaque CAX measurement uncertainty	5.4%	
Total plaque off-axis measurement uncertainty	6.7%	

### III. RESULTS

#### III.A. Gafchromic<sup>®</sup> EBT3 film and single <sup>125</sup>I seed (model 6711)

The single seed EBT3 film measurements were compared to calculated doses from PS and RADCALC<sup>®</sup> for a given exposure time at two depths. PS and RADCALC<sup>®</sup> had previously been shown to agree with hand calculations using TG-43U1 data to within 1% for a single model 6711 I-125 seed<sup>18</sup>.

Agreement between the single seed EBT3 film measurements with calculated doses from PS and RADCALC<sup>®</sup> were within 1.5%. The results are summarised in Table III.

TABLE III. Single seed EBT3 film measured dose comparison with calculated doses.

Depth (mm)	EBT3 Film (Gy)	PS (Gy)	RADCALC <sup>®</sup> (Gy)
2.51	$1.21 \pm 0.07$	1.224	1.220
4.51	$0.41 \pm 0.03$	0.403	0.402

### III.B. Gafchromic® EBT3 film and uniformly loaded ROPES eye plaques

#### III.B.1. Central axis depth dose

The CAX depth dose distributions for uniformly loaded ROPES eye plaques, as measured using EBT3 film are presented in Table IV. Measured CAX depth doses are given without the plaque stainless steel backing as compared with those calculated by both PS and RADCALC®. As shown in Table II, the average total uncertainty in the CAX depth dose measurements was 5.4%.

Using the data in Table IV, it was found that the average reduction in dose on CAX due to the stainless steel backing across all of the ROPES plaques at each depth of measurement was  $0.96 \pm 0.01$  ( $k=1$ ). This value was then entered into PS as a single dose correction factor  $T = 0.96$  and the dose to each point of measurement recalculated. This dose is shown in Table IV as PS Hetero, and is observed to have good agreement with the film measurements in which the stainless steel backing was left on. Agreement is also observed between the film measurements without the stainless steel backing and the full homogeneous water calculations (PS Homo and RADCALC®), this indicates that the acrylic seed carrier has a negligible effect on the CAX depth dose.

TABLE IV. EBT3 film measured and calculated CAX depth dose (Gy) for uniformly loaded ROPES eye plaques. The measurement depths are given from the origin of the eye plaque to the centre of the EBT3 film, as shown in Figure 3.

Plaque	Depth (mm)	PS	RADCALC®	Film (no backing)	Film (with backing)	PS
		Homo				Hetero
10 mm	1.11	1.943	1.943	$1.95 \pm 0.15$	$1.87 \pm 0.15$	1.865
	3.11	1.133	1.137	$1.14 \pm 0.06$	$1.08 \pm 0.06$	1.088
	5.11	0.689	0.695	$0.68 \pm 0.04$	$0.66 \pm 0.04$	0.661
	7.11	0.446	0.450	$0.45 \pm 0.02$	$0.43 \pm 0.02$	0.428
	9.11	0.304	0.307	$0.30 \pm 0.02$	$0.29 \pm 0.02$	0.292
15 mm	1.11	1.944	1.944	$1.92 \pm 0.14$	$1.83 \pm 0.14$	1.866
	3.11	1.194	1.198	$1.17 \pm 0.05$	$1.12 \pm 0.06$	1.146

15 mmN	5.11	0.771	0.777	$0.78 \pm 0.04$	$0.75 \pm 0.04$	0.740
	7.11	0.517	0.521	$0.51 \pm 0.02$	$0.49 \pm 0.02$	0.496
	9.11	0.360	0.362	$0.36 \pm 0.02$	$0.35 \pm 0.02$	0.346
	1.11	1.949	1.949	$1.93 \pm 0.14$	$1.85 \pm 0.14$	1.871
	3.11	1.236	1.240	$1.23 \pm 0.06$	$1.17 \pm 0.06$	1.187
18 mm	5.11	0.805	0.816	$0.80 \pm 0.04$	$0.77 \pm 0.04$	0.773
	7.11	0.541	0.545	$0.54 \pm 0.02$	$0.52 \pm 0.02$	0.519
	9.11	0.376	0.383	$0.37 \pm 0.02$	$0.36 \pm 0.02$	0.361
	1.11	1.967	1.970	$1.93 \pm 0.14$	$1.89 \pm 0.14$	1.888
	3.11	1.418	1.429	$1.41 \pm 0.07$	$1.36 \pm 0.07$	1.361
	5.11	1.003	1.020	$1.01 \pm 0.05$	$0.97 \pm 0.05$	0.963
	7.11	0.714	0.729	$0.70 \pm 0.03$	$0.68 \pm 0.03$	0.685
	9.11	0.516	0.527	$0.51 \pm 0.02$	$0.48 \pm 0.02$	0.495

Using the results from Table IV, along with the heterogeneity correction determined for PS, a table of CAX dose values for ROPES plaques loaded with uniform activity model 6711 I-125 seeds was calculated without and with the steel backing correction, and is shown in Table V. The table displays the CAX depth doses for the eye plaques with seed coordinates given in Table I, with the dose normalised to 85 Gy at 4 mm depth for the homogeneous dose calculation.

TABLE V. CAX dose values (Gy) of the homogeneous and heterogeneous calculations for the four ROPES plaques investigated in this study, with the homogeneous dose normalized to 85 Gy at 4 mm depth for each plaque. Data are for the ROPES plaques uniformly loaded with model 6711 I-125 seeds and the depths are given from the origin of the eye plaque as shown in Figure 3.

Depth (mm)	PS Homo				PS Hetero			
	10 mm	15 mm	15 mmN	18 mm	10 mm	15 mm	15 mmN	18 mm
-1	286.50	288.55	257.79	169.39	275.04	277.01	247.48	162.61
0	239.46	227.37	211.00	158.54	229.88	218.28	202.56	152.20

1	187.61	173.89	167.05	139.80	180.11	166.93	160.37	134.21
2	143.56	134.95	132.53	119.58	137.82	129.55	127.23	114.80
3	109.82	106.46	105.80	101.02	105.43	102.20	101.57	96.98
4	85.00	85.00	85.00	85.00	81.60	81.60	81.60	81.60
5	66.75	68.59	68.80	71.50	64.08	65.85	66.05	68.64
6	53.21	55.84	56.10	60.21	51.08	53.61	53.86	57.80
7	43.04	45.88	46.14	50.84	41.32	44.04	44.29	48.81
8	35.29	38.07	38.29	43.10	33.88	36.55	36.76	41.38
9	29.29	31.85	32.04	36.68	28.12	30.58	30.76	35.21
10	24.57	26.88	27.05	31.38	23.59	25.80	25.97	30.12
11	20.83	22.87	23.01	26.98	20.00	21.96	22.09	25.91
12	17.81	19.61	19.73	23.33	17.10	18.83	18.94	22.40
13	15.34	16.92	17.02	20.27	14.73	16.24	16.34	19.50
14	13.31	14.69	14.78	17.70	12.78	14.10	14.19	16.99

---

### III.B.3. Off-axis profiles

Off-axis dose was measured at each of the 2 mm depth increments given in Table IV. Measured off-axis dose at the most clinically relevant depth of 5.11 mm plotted against off-axis distance for each of the four types of ROPES plaques, are shown in Figures 4(a) to 4(d). The PS Homo curve shows the PS calculated dose for a full homogeneous water assumption, whereas the PS Hetero curve shows the PS calculated dose with the  $T = 0.96$  dose correction factor included, as well as the three-dimensional modelling of the plaque backing.

Agreement is again observed between the film measurement without the stainless steel backing and the dose to water calculations, verifying that the acrylic seed carrier also has a negligible effect on the dose off-axis as well as on the plaque CAX. The global dose correction factor of  $T = 0.96$  is also observed to produce satisfactory agreement with the off-axis measured dose with the stainless steel backing left on.

The effect of the three-dimensional model of the plaque backing is shown in Figures 4(a), 4(b) and 4(c) where a sharp drop in dose occurs near the plaque periphery. This is due to the collimating lip of the eye plaque, which consists of a cylindrical segment connected to the spherical shell of the plaque backing, as shown in Figure 3. The effect of the collimating lip in the three-dimensional model of the plaque was observed to decrease with increasing depth. In order to calculate the dose correctly in this region, it is therefore essential that the dimensions of the plaque backing be modelled precisely in the planning system. This region is of particular interest when attempting to quantify the dose received by organs at risk during plaque therapy. The plaque backing dimensions and compositions used in the planning system should be cross-checked with engineering drawings and technical data provided by the manufacturer.

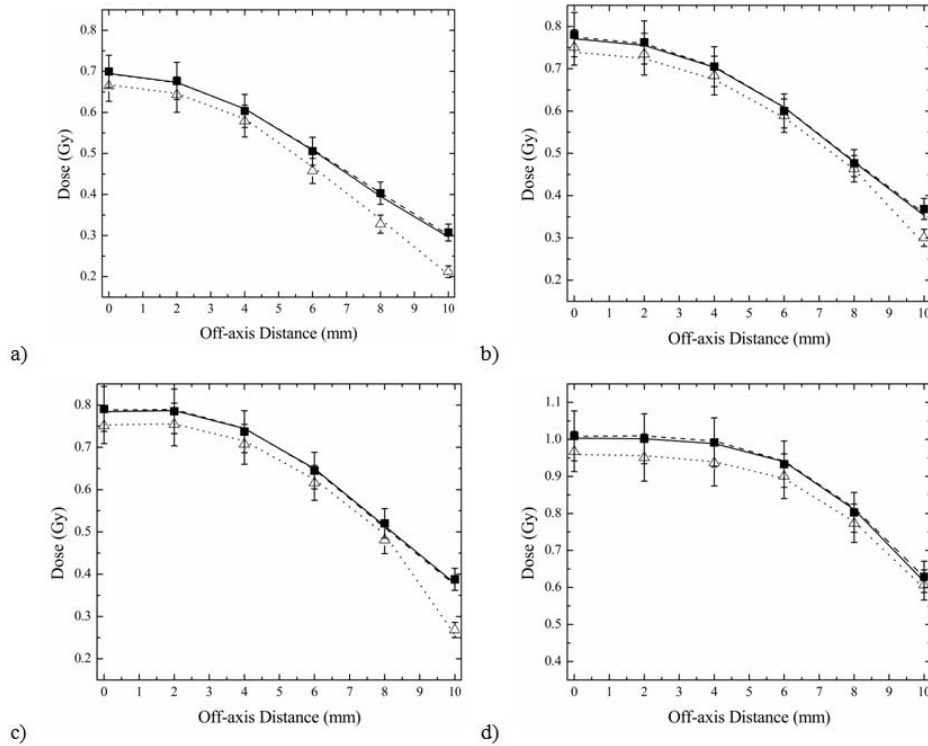


FIG. 4. Off axis profiles at 5.11 mm depth for the a) 10 mm ROPES plaque, b) 15 mm ROPES plaque, c) 15 mm notched ROPES plaque, d) 18 mm ROPES plaque. Dose calculated are represented with lines and dose measured with symbols: RADCALC (dashed lines), PS Homo (solid line), Film without backing (closed square), PS Hetero (dotted line) and Film with backing (open triangle). Errors bars represent the standard deviation of film results ( $k=1$ ).

#### IV. DISCUSSION

The agreement between measured and calculated doses for the single seed experiments confirmed the accuracy of the measurement method using EBT3 film in Solid Water<sup>TM</sup>, as well as the calibration method with the orthovoltage unit.

EBT3 film measurements without the stainless steel backing have been shown to agree with full dose to water calculations, indicating that the acrylic seed carrier has a negligible effect on the dose compared to a full dose to water assumption. Granero *et al.*<sup>17</sup> and Saidi *et al.*<sup>16</sup> have performed Monte Carlo simulations of the 15 mm diameter ROPES plaque, both with and without the acrylic seed carrier to assess its effect on the dose distribution. It was also found in these studies that the acrylic carrier had a negligible effect on the dose distribution.

Granero *et al.*<sup>17</sup> also found a uniform dose reduction of 4% due to the stainless steel plaque backing in the Monte Carlo study for the 15 mm diameter ROPES plaque with model 6711 I-125 seeds. This is in agreement with the dose correction factor of  $T = 0.96 \pm 0.01$  ( $k=1$ ) found using the EBT3 film measurements in this study. With a heterogeneity correction factor  $T = 0.96$  enabled in PS, the material heterogeneity effect of the stainless steel backing could be modelled to match the EBT3 film measurements accurately in three dimensions, within the uncertainty of the measured data to a depth of 10 mm.

Saidi *et al.*<sup>16</sup> found a depth dependent dose correction factor in their Monte Carlo study of two models of Pd-103 seeds in a 15 mm diameter ROPES plaque. A reduction of 4% due to the stainless steel backing was observed at 2 mm depth, and this reduction increased to approximately 9% at 5 mm depth.

When including the three-dimensional model of the plaque backing in PS a sharp drop in dose occurs near the plaque periphery due to the effect of the plaque collimating lip. This effect was also observed in off-axis profile measurements with the stainless steel backing left on. It is in this penumbral region where largest deviations were observed between the measured and predicted doses. These dose differences may be attributed to uncertainties in the film measurements due to positioning uncertainties, or the algorithm used in PS to account for the collimating lip<sup>19</sup>. The effect was also observed by Acar *et al.*<sup>19</sup> in their measurements of the dose distribution produced by COMS plaques using EBT film. Deviations of up to 17% at 5 mm depth and 9% at 12 mm depth occurred between their film measurements and the heterogeneous PS calculation.

Accurate dose calculations are necessary in order to correctly predict the dose to critical structures. It is therefore necessary to model the effect of the eye plaque accurately in three dimensions. However, as noted in AAPM TG-129 report<sup>15</sup>, standardized methods of dose calculation allow multi-institutional analysis of treatment efficacy and side effects. Therefore, the report recommends calculation of both homogeneous (full water medium) and heterogeneous (taking into account the effects of plaque materials) dose distributions. Homogeneous TG-43 dose calculations allow for a comparison of the prescribed dose with patients previously treated at the institution, as well as with other institutions who have historically used the TG-43 dose calculation formalism. Heterogeneous dose calculations allow for a more accurate prediction of the dose delivered to the tumour and surrounding critical structures. The report also included a table of central-axis dose values for fully loaded COMS eye plaques with model 6711 I-125 seeds for both the homogeneous and heterogeneous dose calculations. A corresponding table for ROPES plaques loaded with model 6711 I-125 seeds is included as Table V.

The TG-129 report also recommends an independent check of the dose calculation using either a spreadsheet or third party software. The brachytherapy module of the RADCALC<sup>®</sup> independent checking program has been shown in this study to be appropriate for this purpose and can be used for 3-D dose verification. TG-129 recommends a tolerance of  $\pm 2\%$  on the CAX, the maximum difference observed on the CAX in this study between RADCALC<sup>®</sup> and PS was within this tolerance.

The analysis performed in this study, and that of the TG-129 report, do not consider the effect of tissue heterogeneities within and surrounding the eye. These tissue heterogeneities are likely to further modify the dose distributions from what is observed in conventional TG-43 dose calculations. For example, Thomson *et al.* calculated dose to a number of different eye tissues for I-125 and Pd-103 seeds in various COMS type eye plaques and found differences of up to 9% compared to dose to water calculations<sup>13</sup>. Modern brachytherapy planning systems are introducing model based dose calculation algorithms that will take these tissue heterogeneities into account, and any change in prescribed dose must be carefully examined before introduction of the model based system into the clinical environment. The AAPM/ESTRO/ABS/ABG TG-186 Report has recently been released to address this issue<sup>41</sup>.

## V. CONCLUSION

Dose distributions produced by ROPES type eye plaques loaded with model 6711 I-125 seeds and calculated with Plaque Simulator<sup>TM</sup> without or with correction for the stainless steel backing have been successfully verified with Gafchromic<sup>®</sup> EBT3 film measurements in a Solid Water<sup>TM</sup> eye phantom. The method of dosimetric analysis could be useful in confirming dose distributions predicted by new model based brachytherapy dose calculation algorithms. Measurements performed both on the CAX and off-axis in the absence of the plaque stainless steel backing showed good agreement with homogeneous water dose calculations, indicating that the acrylic seed carrier in ROPES plaques has a negligible effect on the dose distribution, relative to water. Measurements performed with the stainless steel backing showed a uniform decrease of 4% in absolute dose, relative to measurements made without the stainless steel plaque backing. This decrease was observed to be independent of both measurement depth and plaque size. A constant dose correction factor of  $T = 0.96$  was used in PS to account for the effect of the stainless steel plaque backing on the CAX. The three-dimensional model of the plaque, as well as the dose correction factor resulted in an accurate model of the off-axis profiles. Finally, the RADCALC<sup>®</sup> independent checking program was found to agree with PS for a homogeneous water calculation to within 2% on the plaque CAX, and can therefore be considered as appropriate for use as an independent checking program for eye plaque treatment times as recommended in the TG-129 report.

## **ACKNOWLEDGEMENTS**

The authors are thankful to Simon Downes and A/Prof Michael Jackson for their continuing support and financial assistance in the purchase of the specially designed eye phantom. Also, Dr. Wenchang Wong, Dr. Michael Giblin and A/Prof R. Max Conway for their useful discussions on eye plaque episcleral therapy. Finally, the authors would also like to thank Madelaine Tyler for helping with the EBT3 film scanning protocol.

## **REFERENCES**

- <sup>1</sup> R.M. Thomson, and D.W.O. Rogers, "Monte Carlo dosimetry for <sup>125</sup>I and <sup>103</sup>Pd eye plaque brachytherapy with various seed models," Med. Phys. **37**, 368-376 (2010).



- 2 "The Collaborative Ocular Melanoma Study (COMS) randomized trial of pre-enucleation radiation  
of large choroidal melanoma I: characteristics of patients enrolled and not enrolled COMS report no.  
9," *Am. J. Ophthalmol.* **125**, 767-778 (1998).
- 3 C.O.M.S. Group, "Radiation Therapy," in *COMS Manual of Procedures PB95-179693*, edited by  
N.T.I. Service (Springfield, Virginia, 1995).
- 4 B.S. Hawkins, "The collaborative ocular melanoma study (COMS) randomized trial of pre-  
enucleation of large choroidal melanoma: IV. Ten-year mortality findings and prognostic factors.  
COMS Report number 24.," *Am. J. Ophthalmol.* **138**, 936-951 (2004).
- 5 R. Nath, L.L. Anderson, G. Luxton, K.A. Weaver, J.F. Williamson, and A.S. Meigooni, "Dosimetry  
of interstitial brachytherapy sources: Recommendations of the AAPM Radiation Therapy Committee  
Task Group No. 43," *Med. Phys.* **22**, 209-234 (1995).
- 6 S.M. Seltzer, P.J. Lamperti, R. Loevinger, C.G. Soares, and K.A. Weaver, "New NIST air-kerma  
strength standards for I-125 and Pd-103 brachytherapy seeds," *Med. Phys.* **25**, A170 (1998).
- 7 M.J. Rivard, B.M. Coursey, L.A. DeWerd, W.F. Hanson, M.S. Huq, G.S. Ibbott, M.G. Mitch, R.  
Nath, and J.F. Williamson, "Update of AAPM Task Group No. 43 Report: A revised AAPM  
protocol for brachytherapy dose calculations," *Med. Phys.* **31**, 633-674 (2004).
- 8 A. de-la-Zerda, S.-T. Chiu-Tsao, J. Lin, L.L. Boulay, I. Kanna, J.H. Kim, and H.-S. Tsao, "<sup>125</sup>I eye  
plaque dose distribution including penumbra characteristics," *Med. Phys.* **23**, 407-418 (1996).
- 9 S.-T. Chiu-Tsao, L. Bouley, I. Kanna, A. Zerda, and J.H. Kim, "Dose distribution in the eye for Pd-  
103 COMS eye plaque," *Med. Phys.* **22**, 923 (1995).
- 10 A.L. Krintz, W.F. Hanson, G.S. Ibbott, and D.S. Followill, "Verification of plaque simulator dose  
distributions using radiochromic film," *Med. Phys.* **29**, 1220-1221 (2002, abstract).
- 11 A.L. Krintz, W.F. Hanson, G.S. Ibbott, and D.S. Followill, "A reanalysis of the Collaborative Ocular  
Melanoma Study Medium Tumor Trial eye plaque dosimetry," *Int. J. Radiat. Oncol., Biol., Phys.* **56**,  
889-898 (2003).
- 12 S.-T. Chiu-Tsao, L.L. Anderson, K. O'Brien, L. Stabile, and J.C. Liu, "Dosimetry for <sup>125</sup>I seed  
(model 6711) in eye plaques," *Med. Phys.* **20**, 383-389 (1993).
- 13 R.M. Thomson, R.E.P. Taylor, and D.W.O. Rogers, "Monte Carlo dosimetry for <sup>125</sup>I and <sup>103</sup>Pd eye  
plaque brachytherapy," *Med. Phys.* **35**, 5530-5543 (2008).
- 14 C.S. Melhus, and M.J. Rivard, "COMS eye plaque brachytherapy dosimetry simulations for <sup>103</sup>Pd,  
<sup>125</sup>I, and <sup>131</sup>Cs," *Med. Phys.* **35**, 3364-3371 (2008).
- 15 S.-T. Chiu-Tsao, M.A. Astrahan, P.T. Finger, D.S. Followill, A.S. Meigooni, C.S. Melhus, F.  
Mourtada, M.E. Napolitano, R. Nath, M.J. Rivard, D.W.O. Rogers, and R.M. Thomson, "Dosimetry  
of <sup>125</sup>I and <sup>103</sup>Pd COMS eye plaques for intraocular tumors: Report of Task Group 129 by the AAPM  
and ABS," *Med. Phys.* **39**, 6161-6184 (2012).
- 16 P. Saidi, M. Sadehi, A. Shirazi, and C. Tenreiro, "ROPES eye plaque brachytherapy dosimetry for  
two models of <sup>103</sup>Pd seeds," *Australas. Phys. Eng. Sci. Med.* **34**, 223-231 (2011).
- 17 D. Granero, J. Perez-Calatayud, F. Ballester, E. Casal, and J.M. de Frutos, "Dosimetric study of the  
15 mm ROPES eye plaque," *Med. Phys.* **31**, 3330-3336 (2004).
- 18 J. Poder, N. Annabell, M. Geso, M. Alqathami, and S. Corde, "ROPES eye plaque dosimetry:  
commissioning and verification of an ophthalmic brachytherapy treatment planning system," *J.  
Phys.: Conf. Ser.* **444**, 012102 (2013).
- 19 H. Acar, S.-T. Chiu-Tsao, Ozbay, x, smail, G. Kemikler, and S. Tuncer, "Evaluation of material  
heterogeneity dosimetric effects using radiochromic film for COMS eye plaques loaded with <sup>125</sup>I  
seeds (model I25.S16)," *Med. Phys.* **40**, 011708-011713 (2013).
- 20 S.-T. Chiu-Tsao, D. Medich, and J. Munro, "The use of new GAFCHROMIC® EBT film for <sup>125</sup>I  
seed dosimetry in Solid Water® phantom," *Med. Phys.* **35**, 3787-3799 (2008).
- 21 C. Furstoss, B. Reniers, M.J. Bertrand, E. Poon, J.F. Carrier, B.M. Keller, J.P. Pignol, L. Beaulieu,  
and F. Verhaegen, "Monte Carlo study of LDR seed dosimetry with an application in a clinical  
brachytherapy breast implant," *Med. Phys.* **36**, 1848-1858 (2009).
- 22 H. Acar, "Verification of Plaque Simulator dose distributions using GAFCHROMIC EBT film,"  
*Turk Onkoloji Derg.* **25**, 150-156 (2010).
- 23 M.A. Astrahan, G. Luxton, G. Jozsef, T.D. Kampp, P.E. Liggett, M.D. Sapozink, and Z. Petrovich,  
"An interactive treatment planning system for ophthalmic plaque radiotherapy," *Int. J. Radiat.  
Oncol., Biol., Phys.* **18**, 679-687 (1990).
- 24 M.A. Astrahan, "Improved treatment planning for COMS eye plaques," *Int. J. Radiat. Oncol., Biol.,  
Phys.* **61**, 1227-1242 (2005).

25 R.M. Thomson, K.M. Furutani, J.S. Pulido, S.L. Stafford, and D.W.O. Rogers, "Modified COMS  
Plaques for  $^{125}\text{I}$  and  $^{103}\text{Pd}$  Iris Melanoma Brachytherapy," *Int. J. Radiat. Oncol., Biol., Phys.* **78**,  
1261-1269 (2010).

26 C. Dempsey, "Methodology for commissioning a brachytherapy treatment planning system in the era  
of 3D planning," *Australas. Phys. Eng. Sci. Med.* **33**, 341-349 (2010).

27 C. Karolis, C. Amies, R.B. Frost, and F.A. Billson, "The development of a thin stainless steel eye  
plaque to treat tumours of the eye up to 15 mm in diameter," *Australas. Phys. Eng. Sci. Med.* **12**,  
172-177 (1989).

28 J. Dolan, Z. Li, and J.F. Williamson, "Monte Carlo and experimental dosimetry of an  $^{125}\text{I}$   
brachytherapy seed," *Med. Phys.* **33**, 4675-4684 (2006).

29 V. Casanova Borca, M. Pasquino, G. Russo, P. Grosso, D. Cante, P. Sciacero, G. Girelli, M.R. La  
Porta, and S. Tofani, "Dosimetric characterization and use of GAFCHROMIC EBT3 film for IMRT  
dose verification," *J. Appl. Clin. Med. Phys.* **14**, 158-171 (2013).

30 T.A.D. Brown, K.R. Hogstrom, D.A.K.L. Matthews, Ii, K. Ham, and J.P. Dugas, "Dose-response  
curve of EBT, EBT2, and EBT3 radiochromic films to synchrotron-produced monochromatic x-ray  
beams," *Med. Phys.* **39**, 7412-7417 (2012).

31 A.N.-R. Chair, C.R. Blackwell, B.M. Coursey, K.P. Gall, J.M. Galvin, W.L. McLaughlin, A.S.  
Meigooni, R. Nath, J.E. Rodgers, and C.G. Soares, "Radiochromic film dosimetry:  
Recommendations of AAPM Radiation Therapy Committee Task Group 55," *Med. Phys.* **25**, 2093-  
2115 (1998).

32 G. Poludniowski, G. Landry, F. DeBlois, P.M. Evans, and F. Verhaegen, "SpekCalc : a program to  
calculate photon spectra from tungsten anode x-ray tubes," *Phys. Med. Biol.* **54**, N433 (2009).

33 S.C. Klevenhagen, R.J. Aukett, R.M. Harrison, C. Moretti, A.E. Nahum, and K.E. Rosser, "The  
IPEMB code of practice for the determination of absorbed dose for x-rays below 300 kV generating  
potential (0.035 mm Al - 4 mm Cu HVL; 10 - 300 kV generating potential)," *Phys. Med. Biol.* **41**,  
2605-2625 (1996).

34 J.F. Williamson, "Comparison of measured and calculated dose rates in water near I-125 and Ir-192  
seeds," *Med. Phys.* **18**, 776-786 (1991).

35 A.S. Meigooni, S.B. Awan, N.S. Thompson, and S.A. Dini, "Updated Solid Water™ to water  
conversion factors for  $^{125}\text{I}$  and  $^{103}\text{Pd}$  brachytherapy sources," *Med. Phys.* **33**, 3988-3992 (2006).

36 R. Tailor, N. Tolani, and G.S. Ibbott, "Thermoluminescence dosimetry measurements of  
brachytherapy sources in liquid water," *Med. Phys.* **35**, 4063-4069 (2008).

37 H. Chung, B. Lynch, and S. Samant, "High-precision GAFCHROMIC EBT film-based absolute  
clinical dosimetry using a standard flatbed scanner without the use of a scanner non-uniformity  
correction," *J. Appl. Clin. Med. Phys.* **11**, 101-115 (2010).

38 M.J. Butson, T. Cheung, and P.K. Yu, "Evaluation of the magnitude of EBT Gafchromic film  
polarization effects," *Australas. Phys. Eng. Sci. Med.* **32**, 21-25 (2009).

39 L. Menegotti, A. Delana, and A. Martignano, "Radiochromic film dosimetry with flatbed scanners:  
A fast and accurate method for dose calibration and uniformity correction with single film  
exposure," *Med. Phys.* **35**, 3078-3085 (2008).

40 L.A. DeWerd, G.S. Ibbott, A.S. Meigooni, M.G. Mitch, M.J. Rivard, K.E. Stump, B.R. Thomadsen,  
and J.L.M. Venselaar, "A dosimetric uncertainty analysis for photon-emitting brachytherapy sources:  
Report of AAPM Task Group No. 138 and GEC-ESTRO," *Med. Phys.* **38**, 782-801 (2011).

41 L. Beaulieu, A.C. Tedgren, J.-F. Carrier, S.D. Davis, F. Mourtada, M.J. Rivard, R.M. Thomson, F.  
Verhaegen, T.A. Wareing, and J.F. Williamson, "Report of the Task Group 186 on model-based  
dose calculation methods in brachytherapy beyond the TG-43 formalism: Current status and  
recommendations for clinical implementation," *Med. Phys.* **39**, 6208-6236 (2012).